



Editor choice paper

γ -Alumina-supported [60]fullerene catalysts: Synthesis, properties and applications in the photooxidation of alkenes

Manolis D. Tzirakis^a, John Vakros^b, Loukia Loukatzikou^c, Vasilis Amargianitakis^a,
Michael Orfanopoulos^{a,*}, Christos Kordulis^{b,d}, Alexis Lycourghiotis^{b,**}

^a Department of Chemistry, University of Crete, GR-71003 Voutes, Crete, Greece

^b Department of Chemistry, University of Patras, GR-26500 Rio, Patras, Greece

^c Department of Chemistry, University of Ioannina, GR-45110 Ioannina, Greece

^d Institute of Chemical Engineering and High-Temperature Chemical Processes (FORTH/ICE-HT), GR-26500 Patras, Greece

ARTICLE INFO

Article history:

Received 23 June 2009

Received in revised form

30 September 2009

Accepted 1 October 2009

Available online 9 October 2009

Keywords:

C₆₀

Photocatalysis

Singlet oxygen

Photooxidation

DRS

Supported catalysts

Supported C₆₀

Photoluminescence

TGA

Ene reaction

γ -Alumina

γ -Al₂O₃

ABSTRACT

Immobilization of [60]fullerene onto γ -Al₂O₃ surface provides new heterogeneous photocatalysts for the oxidation of organic compounds under oxygen atmosphere. These catalysts have been prepared by simple or successive incipient wetness impregnation (using an organic solvent) followed by air-heating at 180 °C. In the C₆₀/Al₂O₃ system, C₆₀ loading was varied in the range of 1–4% (w/w). Several experimental techniques including BET, XRD, DRS, TGA, microelectrophoresis, photoluminescence and kinetic extraction, have been used to characterize these catalytic materials. It was found that the quite high surface exposed by the supported C₆₀ increases with the amount of the supported C₆₀, while the dispersion of the supported C₆₀ decreases. The quite stable supported [60]fullerene phase is comprised from C₆₀ clusters, small and large aggregates. This non-uniform size distribution is reflected to a non-uniform distribution concerning the 'supported phase-support' interactions. These interactions decrease with the amount of the supported C₆₀. The photocatalysts prepared may be safely used up to 200 °C. Above this temperature the supported C₆₀ is sublimated/combusted in air.

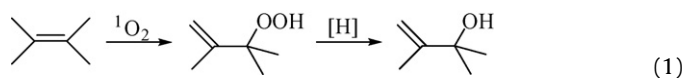
The photocatalytic activity of the so-obtained catalytic systems has been evaluated in terms of substrate conversion in the singlet oxygen 'ene' reaction of alkenes. The photooxygenation of 2-methyl-2-heptene has been examined as a probe reaction. It was found that the catalytic activity increases with the increasing amount of the supported C₆₀ up to the value of 3% (w/w) and then decreases. The intrinsic activity expressed as TON or TOF decreased monotonically with C₆₀. In all cases, however, the photocatalytic activity of the Al₂O₃-supported C₆₀ catalysts was substantially increased compared to the unsupported C₆₀ precursor, exhibiting quantitative conversion yields after short reaction times. The catalytic behavior was attributed to the aforementioned opposite trends which follow the surface exposed by the supported C₆₀ on one hand and the 'supported C₆₀-support' interactions and the C₆₀ dispersion on the other hand. The easy separation of these solid catalysts from the reaction mixture, the high activity and stability as well as the retained activity in subsequent catalytic cycles, make these supported catalysts suitable for a small-scale synthesis.

© 2009 Elsevier B.V. All rights reserved.

1. Introduction

Oxidation is a ubiquitous reaction in synthetic organic chemistry with both academic and industrial relevance. Among the several oxidation protocols reported so far, the photooxidation with singlet oxygen (¹O₂) possesses a rather prominent role [1–5]. The Schenck

'ene' reaction is, unarguably, one of the most interesting modes of reactions of singlet oxygen with organic compounds (Eq. (1)) [6,7]:



The allylic hydroperoxides formed in this reaction are usually immediately reduced to the corresponding allylic alcohols. These compounds have proven to be synthetically useful intermediates in the synthesis of fine chemicals.

Typically, singlet oxygen is produced upon photoexcitation using various sensitizers such as xanthene dyes, porphyrins (i.e.,

* Corresponding author. Tel.: +30 2810545030; fax: +30 2810545001.

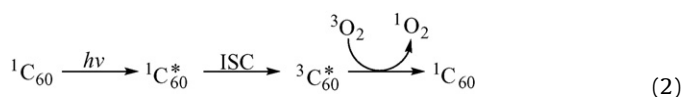
** Corresponding author. Tel.: +30 2610997114; fax: +30 2610994796.

E-mail addresses: orfanop@chemistry.uoc.gr (M. Orfanopoulos),

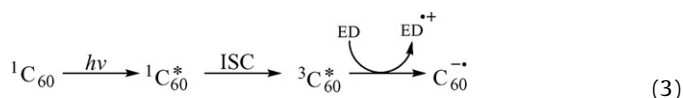
alycour@chemistry.upatras.gr (A. Lycourghiotis).

phthalocyanines), phenothiazines (i.e., methylene blue), and fluoresceins (i.e., rose bengal). These compounds exhibit a high absorption coefficient in the visible region of the spectrum. The role of these sensitizers is to absorb the light and transfer their energy to molecular oxygen in the ground state thereby forming the reactive singlet oxygen. Conventionally, photosensitized reactions are carried out in homogeneous solutions. However, the main shortcoming of a homogeneous system stems from the requirement of separation and recycling of the sensitizer, which is of primary concern in 'green chemistry'. For catalytic oxidations, a 'green' approach is the development of a solid, recyclable catalyst and the use of an environmentally friendly reagent, such as molecular oxygen as the only oxidant. Working at room temperature and atmospheric pressure is also desirable.

[60] Fullerene is a well-established singlet oxygen sensitizer [8–12]. When C_{60} is irradiated with UV/vis light, it is excited from the S_0 ground state to a short-lived (ca. 1.2 ns) singlet excited state (E_S 46.1 kcal/mol) [13]. The singlet excited state (S_1) undergoes rapid intersystem crossing (ISC) at a rate of $5.0 \times 10^8 \text{ s}^{-1}$ to a lower lying triplet state T_1 (E_T 37.5 kcal/mol) with a long lifetime ($>40 \mu\text{s}$) [8,14,15]. In the presence of dissolved molecular oxygen (3O_2), which exists as a triplet in its ground state, the fullerene T_1 state is quenched to generate singlet oxygen (1O_2) by energy transfer at a rate of $2 \times 10^9 \text{ M}^{-1} \text{ s}^{-1}$ (Eq. (2)). The singlet oxygen quantum yield, Φ_Δ , for this process has been reported to be nearly 1.0 (excitation at 532 nm) [8,9]. On the other hand, the reverse process (i.e., quenching of singlet oxygen by ground state fullerene) proceeds at a much smaller rate [8]. This property, in conjunction with the low fluorescence quantum yield, renders [60] fullerene an excellent photosensitizer:



On the other hand, photoexcited fullerenes are also excellent electron acceptors capable of accepting as many as six electrons [16,17]. $^3C_{60}^*$ has a higher electron-accepting ability than ground state $^1C_{60}$, and electron-donating compounds (ED) such as amines can reduce $^3C_{60}^*$ to give the C_{60} radical anion ($^3C_{60}^{\bullet-}$) (Eq. (3)) [18], which may react further (e.g., through radical coupling pathways) [19,20]:



Moreover, electrons may transmit from the conduction band of a semiconductor used in photocatalysis (e.g., TiO_2 , ZnO) into the deposited $^3C_{60}^*$ resulting to the formation of $^3C_{60}^{\bullet-}$. Thus, the supported C_{60} particles on the semiconductor surface act as electron traps. Therefore, it is expected to improve the photocatalytic behavior of these semiconductors [21–29].

In the present study, we extend our interest in heterogeneous photocatalysis [30–32], and report on the synthesis and characterization of a series of Al_2O_3 -supported fullerene catalysts with varying C_{60} content in the range of 1–4% (w/w). Specifically, we investigate the deposition mechanism of C_{60} on the support surface, the state of dispersion and the size distribution of the deposited C_{60} aggregates, the "supported phase-support" interactions and the stability of the active phase against sublimation/combustion. Moreover, we explore the activity, stability and reusability of these supported catalysts in the 1O_2 oxidation of alkenes ('ene' reaction), examining the 2-methyl-2-heptene oxidation as a model reaction. Finally, we attempt to correlate the catalytic activity of

these photocatalysts to their important physicochemical characteristics.

2. Experimental

2.1. Preparation of the supported photocatalysts

The supported $C_{60}(x)$ photocatalysts were prepared by depositing C_{60} on the surface of γ -alumina grains of 100–150 mesh. The x in the above notation denotes the C_{60} content of the photocatalyst (% w C_{60} /w catalyst). It takes the values 1, 2, 3, and 4. The aforementioned nominal values were confirmed by determining experimentally the carbon content. The γ -alumina (specific surface area $231 \text{ m}^2/\text{g}$, specific pore volume 0.76 mL/g) and the C_{60} used were purchased, respectively, from Akzo and Ses Research. The sample with the lowest C_{60} content (1% w C_{60} /w catalyst) was prepared by simple incipient wetness impregnation. The impregnating solution was prepared by dissolving the proper amount of C_{60} in 1,2-dichlorobenzene. Then, the impregnated sample was heated at 180°C for 4 h in air. The remainder samples were prepared by successive wetness impregnations, where each sample was prepared starting from the previous one through the same impregnation procedure mentioned above. Thus, $C_{60}(2)$, $C_{60}(3)$ and $C_{60}(4)$ samples have been prepared starting from $C_{60}(1)$, $C_{60}(2)$ and $C_{60}(3)$, respectively.

2.2. Characterization of the supported photocatalysts

2.2.1. Specific surface area measurements (SSA)

The SSA of the photocatalysts was determined by applying the BET equation and using a flow technique. Pure nitrogen (Linde special) and helium (Linde 99.996%) were used as adsorbate and inert gas, respectively, in a laboratory-constructed apparatus. The amount of nitrogen adsorbed at liquid-nitrogen temperature and at three different partial pressures was determined using a thermal conductivity detector of a gas chromatograph (Varian Series 1700).

2.2.2. X-ray powder diffraction (XRD)

The XRD patterns of the powdered samples were recorded with an ENRAF NONIUS FR 590 diffractometer using $\text{Cu K}\alpha$ (1.54198 \AA) radiation. The generator is equipped with a curved position sensitive detector CPS120 of INEL. This was operated at 45 kV and 25 mA.

2.2.3. Diffuse reflectance spectroscopy (DRS)

The diffuse reflectance spectra of the calcined samples were recorded in the range 200–800 nm at room temperature. A UV-vis spectrophotometer (Varian Cary 3) equipped with an integration sphere has been used. $\gamma\text{-Al}_2\text{O}_3$ was used as a reference. The powdered samples were mounted in a quartz cell. This provided a sample thickness greater than 3 mm to guarantee the "infinite" sample thickness.

2.2.4. Photoluminescence (PL)

The Photoluminescence spectra of the samples studied were recorded at room temperature in air using a SHIMADZU RF-5301 spectrofluorophotometer equipped with a 150 W xenon lamp, a red sensitive photomultiplier and reflection grating monochromators with fixed slits of 3 nm. The wavelength accuracy was $\pm 1.5 \text{ nm}$. A long-wavelength passing filter (UV-35) was used on the emission monochromator side to cut off the scattered and the second order lights.

2.2.5. Microelectrophoresis

The ζ potential of the solid particles was measured at 25 °C using a Zetasizer 5000 (Malvern Instruments Ltd.) microelectrophoresis apparatus. Sufficiently dilute aqueous suspensions of a given sample were prepared with constant ionic strength, 0.01 M. The pH of the suspensions was adjusted by adding small amounts of 1 M HNO₃ or KOH solution. The ' ζ potential vs. pH' curves were thus obtained. The pH value at which the ζ potential takes a zero value was identified as the isoelectric point of the sample (IEP).

2.2.6. Thermogravimetric analysis (TGA)

The TGA of the samples was carried out under He atmosphere using a DuPont thermo-balance. In all experiments the sample temperature was increased from 25 to 700 °C with a rate of 10 °C min⁻¹. From these spectra the corresponding differential spectra have been derived.

2.2.7. Carbon determination in the solid samples

The amount of carbon contained in the solid samples was determined using a Carlo Erba CHN analyzer (EA 1108, Elemental Analyzer).

2.2.8. C₆₀ extraction experiments

Kinetic C₆₀ extraction experiments were performed in order to investigate the magnitude of interactions between the supported C₆₀ phases and the support surface. In each experiment an amount of the sample was immersed in a volume of 1,2-dichlorobenzene fifteen times greater than the pore volume of the sample. The amount of the extracted C₆₀ was then determined photometrically at various times in the range 0–5600 min.

2.3. Photooxygenation tests

2.3.1. Analytical techniques

¹H NMR and ¹³C NMR spectra were recorded on Bruker AMX-500 MHz (125 MHz for ¹³C) and DPX-300 MHz (75 MHz for ¹³C) spectrometers, in CDCl₃. Chemical shifts are reported in ppm relative to TMS using the residual solvent signals at 7.26 and 77.16 ppm as internal references for the ¹H and ¹³C spectra, respectively. GC–MS analysis was performed on a Shimadzu GC MS-QP5050A apparatus equipped with a Supelco capillary column (MDN-5, 30m × 0.25 mm × 0.25 μm film thickness) and CI mass detector (5971A MS). Gas chromatographic analyses were performed on a Hewlett Packard 5890 series II instrument, equipped with HP silica fused capillary column (20% permethylated β-cyclodextrin, 30m × 0.25 mm I.D. × 0.25 μm film thickness). UV–vis spectra were recorded on a Shimadzu MultiSpec-1501 UV/Visible spectrophotometer.

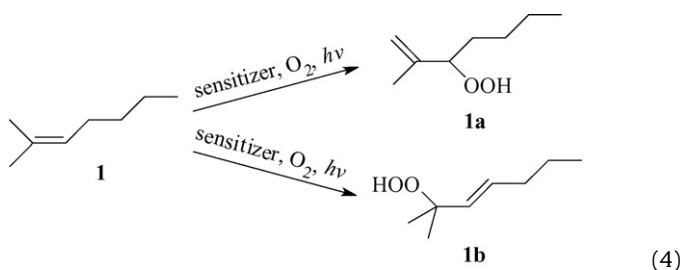
2.3.2. Solvents and reagents

Commercially available solvents or reagents were used as received without further purification. Acetonitrile HPLC-grade was used as the reaction solvent. 2-Methyl-2-heptene was prepared in 50% yield by Wittig reaction of isopropyltriphenylphosphorane with pentanal and purified by fractional vacuum distillation. The final product was characterized by ¹H and ¹³C NMR spectroscopy, as well as by mass spectrometry. ¹H NMR (500 MHz, CDCl₃): 0.90 (t, 3H), 1.32 (m, 4H), 1.61 (s, 3H), 1.70 (s, 3H), 1.98 (m, 2H), 5.13 (t, 1H); ¹³C NMR (500 MHz, CDCl₃): δ 14.16, 17.76, 22.55, 25.85, 27.93, 32.30, 125.08, 131.23; MS: *m/z* = 112 (M – 43, 69).

2.3.3. Photocatalytic reactions

The model reaction (Eq. (4)) was carried out in 4 mL glass vial sealed with a Teflon-coated silicone septum. This reaction follows

a parallel kinetic scheme:



The reaction solution (CH₃CN, 1 mL) contained 0.03 M of 2-methyl-2-heptene and 3.6 mg of Al₂O₃-supported C₆₀ catalyst. The corresponding unsupported C₆₀ was also evaluated under the same conditions, for comparison purposes. In this case the concentration of C₆₀ in the reaction mixture was 2 × 10⁻⁴ M, corresponding to that involved in the suspension of the C₆₀(4) photocatalyst.

The solution was irradiated under a constant stream of molecular oxygen at 0–5 °C. A Cermax 300 W Xenon lamp (with UV-filter output that covers a broad spectral range ~390–770 nm) was used as the light source. The insoluble catalyst was kept in suspension by vigorous magnetic stirring. During irradiation, aliquots of the reaction mixture were pooled out, the solid materials were filtered-off, Ph₃P was added (to reduce the allylic hydroperoxides to the corresponding alcohols) and the resulting sample was left at RT for 20 min. GC and/or GC–MS analysis was used to monitor the reaction over time. *n*-Nonane was used as internal standard.

The % conversion values reported are the average of three measurements obtained from three separate experiments performed for each catalyst. The molar ratio **1a** and **1b** was determined by ¹H NMR spectroscopy.

The turnover number (TON) was calculated by dividing the concentration of products **1a** and **1b** (mol of products) with the amount of the supported C₆₀ (mol of C₆₀). The turnover frequency (TOF) was calculated by dividing TON with time (s).

3. Results and discussion

3.1. The texture of the photocatalysts and the estimated size of the supported C₆₀ clusters/aggregates

Table 1 compiles the values of the specific surface area (SSA) of both the γ-Al₂O₃ support (after pore volume impregnation with pure solvent followed by air-heating at 180 °C for 4 h) and the C₆₀(*x*) photocatalysts (*x* = 1, 2, 3, 4). The deposition of the minimum amount of C₆₀ does not bring about any change in the SSA. This indicates that the deposited C₆₀ does not actually disturb the alumina porous structure by extending pore blocking. This is a first indication that in this sample quite small C₆₀ aggregates and/or molecular C₆₀ clusters are formed on the support surface. Increase in the C₆₀ loading causes a rather small decrease in the SSA indicating a rather small decrease in the C₆₀ dispersion with the amount of the supported phase. These conclusions are further confirmed by the X-ray diffraction patterns (not shown here). In fact, the XRD diffraction pattern of γ-alumina is observed in all cases (main

Table 1

Values of the specific surface area (SSA), the isoelectric point (IEP) and the percentage surface area exposed by the supported C₆₀ (% X_{C₆₀}).

Catalysts	SSA (m ² g ⁻¹)	IEP.	% X _{C₆₀}
γ-Al ₂ O ₃	231	8.8	–
C ₆₀ (1)	234	8.5	7.3
C ₆₀ (2)	206	8.4	9.8
C ₆₀ (3)	212	8.3	12.2
C ₆₀ (4)	191	8.2	14.6

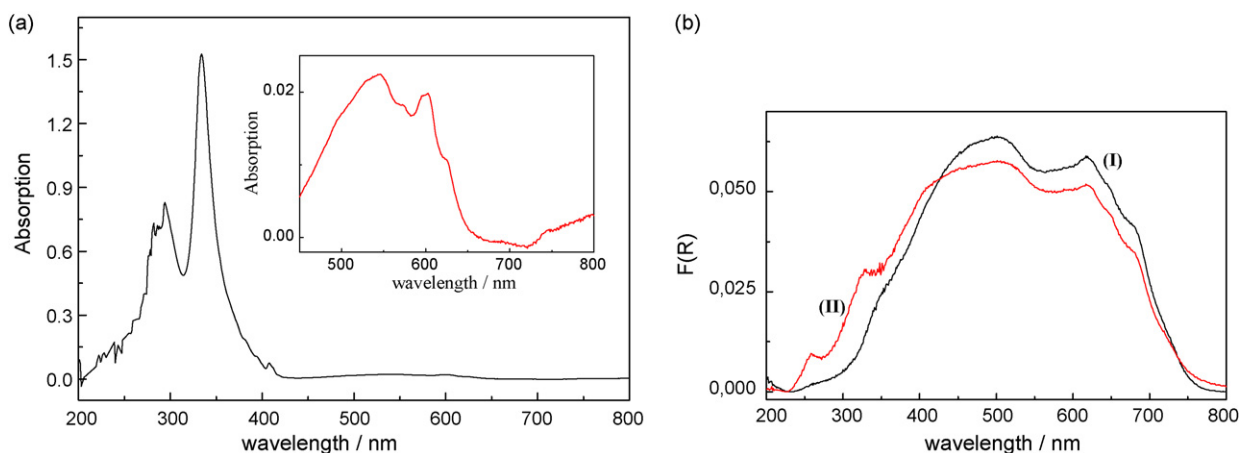


Fig. 1. (a) Absorption spectrum of a C_{60} solution in 1,2-dichlorobenzene. (b) DR spectra of a mechanical mixture of C_{60} with γ -alumina (2%, w/w) before (I) and after (II) heating at 180 °C for 4 h.

diffraction peaks at 2θ equal to 66.7° and 45.8°). Only the maximum C_{60} peak at $2\theta = 21.8^\circ$ is hardly visible in the XRD spectra of the two photocatalysts with the higher C_{60} loading.

3.2. The dispersive action of the γ -alumina surface

The dispersive action of the γ -alumina surface is better revealed by studying the electronic spectra of: (i) C_{60} in 1,2-dichlorobenzene (Fig. 1a), (ii) a mechanical mixture of the solid C_{60} with γ -alumina surface before and after drying at 180 °C for 4 h (Fig. 1b), and (iii) the prepared photocatalysts (Fig. 2).

In the UV–vis absorption spectrum of the dissolved C_{60} appear two strong absorption peaks (284, 335 nm) in the ultraviolet region, a small peak at 410 nm and a very weak extended band in the visible region. The peaks are mainly attributed to the C_{60} molecules/clusters or very small aggregates whereas the weak band to the C_{60} relatively large aggregates. A magnification of the spectrum in the visible region is illustrated in the inset of Fig. 1a. Inspection of this picture shows that the large band (475–650 nm) is rather structured involving four peaks at about 525, 550, 600 and 625 nm. The aforementioned peaks in the ultraviolet and visible region are in good agreement to those reported in the literature [33–35]. In order to confirm that the absorption in this region is actually due to the C_{60} relatively large aggregates we have taken the diffuse reflectance spectrum of a mechanical mixture of C_{60} and γ -alumina (Fig. 1b, curve I) because it is well known that the

grains of solid C_{60} are comprised from C_{60} aggregates. In this spectrum an extended band appears in the range 400–700 nm whereas the absence of bands at 284, 335 nm indicates the absence of C_{60} molecules/clusters or very small C_{60} aggregates. The heating of the mechanical mixture at 180 °C for 4 h increases the supported fullerene/ γ -alumina interactions resulting to somewhat better dispersion of the supported C_{60} . This is manifested by the increase (decrease) of the $F(R)$ value in the range 250–400 nm (440–700 nm) (Fig. 1b, II).

The excellent dispersing ability of the γ -alumina surface is much more pronounced in the supported photocatalysts. In fact, inspection of Fig. 2 clearly shows that a large portion of the supported C_{60} is comprised from C_{60} clusters or very small C_{60} aggregates which are manifested by the peaks centered at about 260 nm and 335 nm. The remained portion of the supported C_{60} is comprised from aggregates of progressively increasing size. The relatively small aggregates absorb in the range 350–450 nm whereas the larger ones in the range 450–650 nm. Thus, the application of the diffuse reflectance spectroscopy reveals not only the excellent dispersing ability of the γ -alumina surface but the non-uniform size distribution of the supported C_{60} clusters/aggregates as well.

The dispersive action of γ -alumina has been also investigated by photoluminescence. The photoluminescence spectra of γ -alumina, solid C_{60} , the catalysts studied and a mechanical mixture containing 2% (w/w) C_{60} and 98% (w/w) γ -alumina are illustrated in Fig. 3.

These spectra were recorded after excitation at 220 nm. It may be seen that both materials emit at similar wavelengths [C_{60} (γ -alumina): 365(375), 470(450–550), 724(725) and 826(826)]. In all cases the γ -alumina peaks are much more intense than the corresponding ones of the C_{60} .

Because photoluminescence often originates near the surface of a material [36] it constitutes an important technique for the characterization of surfaces [37]. Moreover, the presence of species deposited on a surface alters the intensity of the photoluminescence signal. Several studies on the photoluminescence of C_{60} have shown that the number and the location of the peaks depend on the size of the C_{60} entities (i.e., small nanoparticles, clusters of nanoparticles, bigger aggregates), the crystallinity of the material, the temperature at which the spectra have been recorded and the topochemical environment [38–41]. Thus, the assignment of the various peaks at particular C_{60} entities is quite difficult though the peaks observed by us are in reasonable agreement with those found in the literature [38–41]. Concerning the γ -alumina, two emission peaks at 343 and 378 nm as well as a broad band centered at 500 nm have been reported for photoluminescence spectra recorded in the range 300–700 nm. The peaks were attributed to the F^+ center,

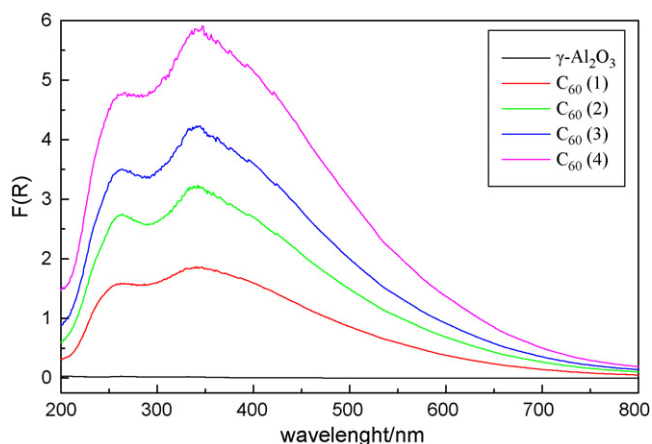


Fig. 2. DR spectra of the support (after treatment with 1,2-dichlorobenzene and heating at 180 °C for 4 h) and the catalysts prepared.

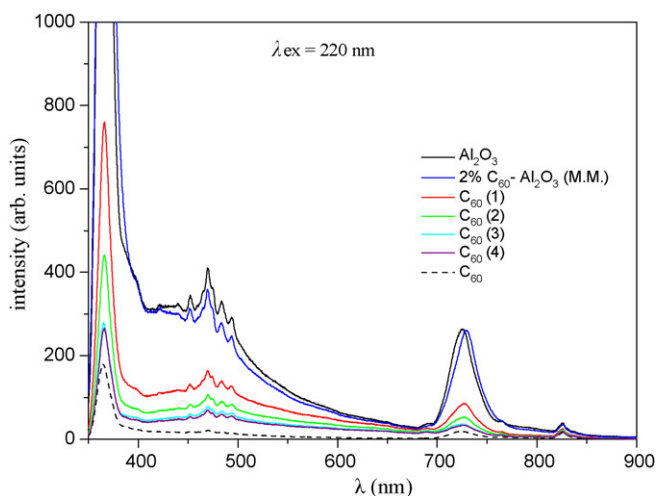


Fig. 3. Emission spectra recorded in the range 350–900 nm for the γ -alumina, the solid C_{60} , the catalysts studied and a mechanical mixture. The materials were excited at $\lambda_{\text{ex}} = 220$ nm.

while the broad band was attributed to impurities [42]. One of these peaks and the broad band has been also detected in our spectra.

In spite of the aforementioned difficulties to assign all the peaks detected in the photoluminescence spectra obtained in the present work, these are very useful for investigating the dispersive action of γ -alumina. The decrease in the intensity of the γ -alumina peaks due the presence of the C_{60} is much more pronounced in the sample $C_{60}(2)$ than in the mechanical mixture containing the same amount of C_{60} (Fig. 3). This has been observed for all the catalysts studied and the corresponding mechanical mixtures and shows that the deposited C_{60} is dispersed quite well covering a considerable portion of the γ -alumina surface. The surface coverage increases with the C_{60} content as it may be deduced by the observation that the aforementioned decrease in the intensities of the peaks increases with the C_{60} content in the catalysts.

3.3. The surface exposed by the supported C_{60}

Taking into account the above it would be interesting to investigate further the dispersive action of the γ -alumina surface by determining the surface exposed by the supported C_{60} . This may be estimated by determining the values of the IEP for the γ -alumina ($\text{IEP}_{\text{Al}_2\text{O}_3}$) the solid (C_{60} , $\text{IEP}_{C_{60}}$) and the photocatalysts studied ($\text{IEP}_{C_{60}^x}$). Provided that the ‘support–supported phase’ interactions do not affect considerably the *acid–base behavior* of the γ -alumina and the supported C_{60} , the above parameters are related by the following relationship [43]:

$$X_{C_{60}} \cdot \text{IEP}_{C_{60}} + X_{\text{Al}_2\text{O}_3} \cdot \text{IEP}_{\text{Al}_2\text{O}_3} = \text{IEP}_{C_{60}^x} \quad (5)$$

where $X_{C_{60}}$ and $X_{\text{Al}_2\text{O}_3}$ stand for the fractions of the surface of each photocatalyst exposed by the supported C_{60} and the bare support, respectively. On the other hand it is obvious that

$$X_{C_{60}} + X_{\text{Al}_2\text{O}_3} = 1 \quad (6)$$

By combining the above equations we may derive the following relationship:

$$X_{C_{60}} = \frac{\text{IEP}_{C_{60}^x} - \text{IEP}_{\text{Al}_2\text{O}_3}}{\text{IEP}_{C_{60}} - \text{IEP}_{\text{Al}_2\text{O}_3}} \quad (7)$$

The values obtained for the isoelectric point are compiled in Table 1. As expected [43], there is a shift of these values from $\text{IEP}_{\text{Al}_2\text{O}_3} = 8.8$ to $\text{IEP}_{C_{60}} = 4.7$. The application of Eq. (7) allowed the determination of $X_{C_{60}}$ values (Table 1). Using these values and the

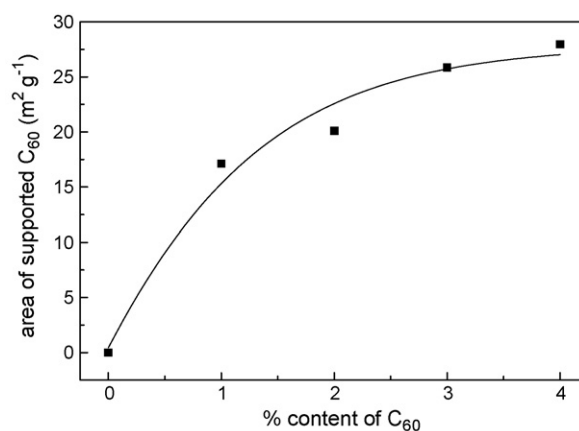


Fig. 4. Variation of the area exposed by the supported C_{60} with the loading of C_{60} in the photocatalysts studied.

corresponding values for the SSA (Table 1) we have calculated the specific surface area exposed by the supported C_{60} . The variation of this area with the C_{60} content is illustrated in Fig. 4. It may be seen that this area is rather large indicating a quite high dispersion of the supported C_{60} , in agreement with the DRS, XRD and PL results. Moreover, it may be observed that this area increases with increasing C_{60} loading, while the dispersion of the supported C_{60} decreases. The latter suggests that the size distribution of the supported C_{60} clusters/aggregates, inferred by DRS, shifts to higher values as the loading increases. This is also in line with the aforementioned BET and XRD results.

3.4. Support–supported phase interactions

The non-uniform size distribution of the supported C_{60} could reflect a similar profile with respect to the magnitude of interactions of the supported C_{60} phases with the γ -alumina surface. This was investigated by performing kinetic C_{60} extraction experiments. The kinetics of the C_{60} extraction in 1,2-dichlorobenzene is illustrated in Fig. 5.

It may be seen that a portion of the supported C_{60} (ca. 30%) is extracted within 30 min. This may concern the relatively large, and thus loosely bound C_{60} aggregates which absorb in the range 450–650 nm in the DRS spectra (Fig. 2). A large period of time (ca. 5600 min) is required for a second portion of supported C_{60} to be extracted (ca. 30%). This could correspond to the relatively small

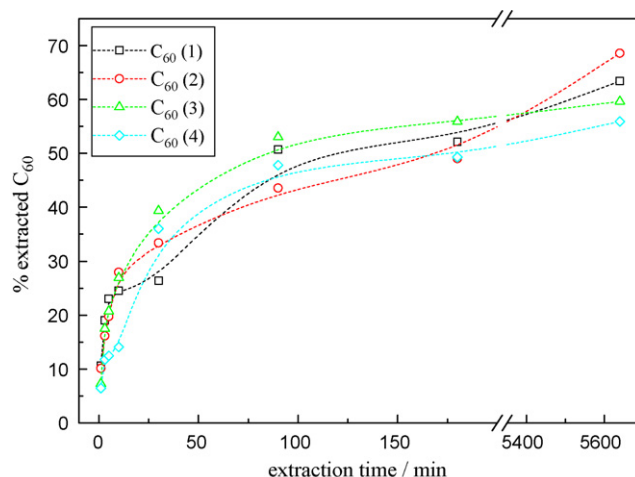


Fig. 5. Kinetics of the extraction of C_{60} from the catalysts prepared.

aggregates absorbing in the range 350–450 nm in the DRS spectra (Fig. 2). Moderate support–supported phase interactions are expected in this case. Finally, another portion of the supported C_{60} (ca. 40%) remains on the support surface even after 5600 min. This could correspond to the C_{60} clusters or very small C_{60} aggregates, which are manifested by the peaks centered at about 260, and 335 nm in the DRS spectra (Fig. 2). Thus the kinetics of the C_{60} extraction corroborated the picture for the supported C_{60} drawn from the other characterization techniques, mainly from the DR spectroscopy. However, this kinetics is not sufficiently sensitive to reveal details concerning the effect of the C_{60} loading on the ‘support–supported phase’ interactions.

A more suitable tool to probe these interactions is proved to be photoluminescence. In fact, a very interesting observation in the photoluminescence spectra is the presence of an additional broad emission band centered at around 550 nm in the spectra recorded after excitation at 340, 350, 476 and 488 nm for the catalysts studied. A part of these spectra, recorded after excitation at 350 nm, is illustrated in Fig. 6. The band at 550 nm does not appear in the photoluminescence spectra recorded for the γ -alumina, C_{60} and the mechanical mixtures. Actually, the emission spectrum of the γ -alumina illustrated in Fig. 6 is simply the tail of the band centered at about 470 nm (see also Fig. 3).

The appearance of the band at 550 nm may be attributed to the quite strong interactions between the well-dispersed C_{60} and the γ -alumina surface, which change the local topochemical environment of the supported C_{60} . *It may be seen that these interactions decrease with increasing the C_{60} loading.* This observation is in line with the aforementioned finding that the dispersion of the supported C_{60} decreases as the C_{60} loading increases. As we shall see both effects are important for explaining the intrinsic catalytic behavior of the supported photocatalysts.

3.5. Stability of the supported phase against sublimation/combustion

It is well known that above a critical temperature the solid C_{60} is sublimated and/or combusted in air. Thus, another critical point concerning the preparation of functional C_{60} -based photocatalysts is the determination of the temperature range at which the developed photocatalysts are stable. The differential version of the TGA curves can help us to investigate this point. These curves are illustrated in Fig. 7.

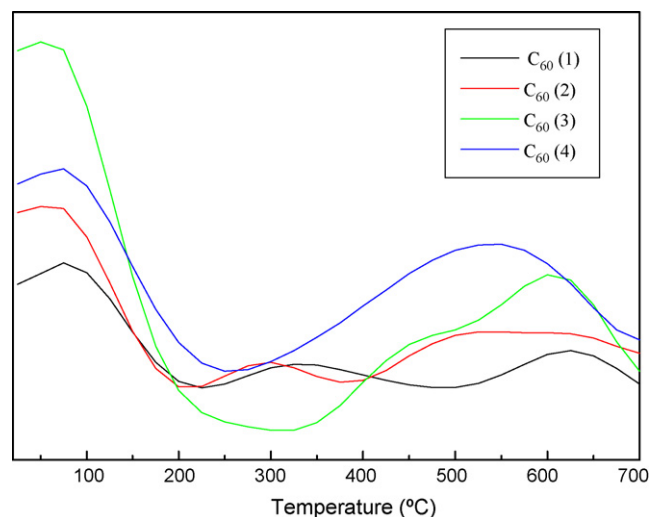


Fig. 7. Differential TGA curves derived under ambient atmosphere for the catalysts prepared.

It may be seen that there are two temperature ranges in which a loss of weight is observed. The first centered at about 70 °C concerns the removal of the surface water molecules. The second quite wide range (230–750 °C) concerns the progressive sublimation/combustion of the supported C_{60} . This shows that the prepared photocatalysts could be safely used up to 200 °C. On the other hand the broadness of the second range and the appearance of one or two peaks within this range may reflect the non-uniform distribution concerning the size of the supported C_{60} clusters/aggregates and their interactions with the support surface. An interesting observation is that the maximum of the differential TGA curves appeared above 500 °C, which presumably correspond to more strongly interacted C_{60} supported species with the support surface, shifts to lower temperatures with increasing C_{60} loading. This is in line with the PL and microelectrophoresis findings that the ‘ C_{60} -alumina’ interactions and the C_{60} dispersion decrease with increasing the C_{60} loading.

3.6. On the mechanism of formation of the supported C_{60}

The method used for the preparation of the supported photocatalysts involved two steps: the incipient wetness impregnation and the heating step. It will be interesting to investigate at which of these steps the deposition takes place. In order to investigate this point we have selected the sample with the minimum C_{60} content, because it was the only one prepared by simple incipient wetness impregnation. The DR spectra of this specimen recorded after impregnation and after heating are illustrated in Fig. 8. The corresponding spectra recorded for the support are illustrated in the inset of this figure.

Comparison of the spectrum of the wet sample with the DR spectrum of the support impregnated with the pure solvent and with the absorption spectrum of the C_{60} molecules in a solution of 1,2-dichlorobenzene (Fig. 1a) clearly shows that the DR spectrum of the wet C_{60} (1) specimen is simply the combination of these two spectra. This strongly suggests that upon impregnation, C_{60} molecules or small clusters are simply transferred inside the pores of the support and that *there are not any specific interactions of these species with the support surface.* Thus, in our case the porous of the support act as simple reservoirs for the fullerene species. It is in the heating step where the solvent is removed and the C_{60} species are deposited on the support surface. These are respectively manifested by the disappearance of the DR spectrum of the solvent (inset of

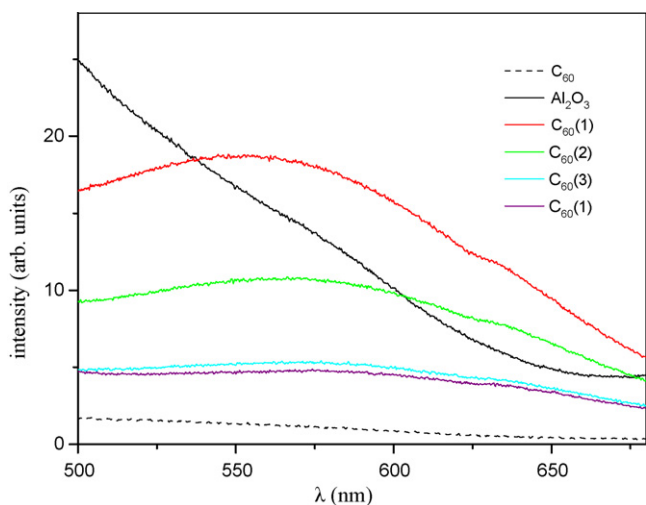


Fig. 6. Emission spectra recorded in the range 500–700 nm for the γ -alumina, the solid C_{60} and the catalysts studied ($\lambda_{\text{excitation}} = 350$ nm).

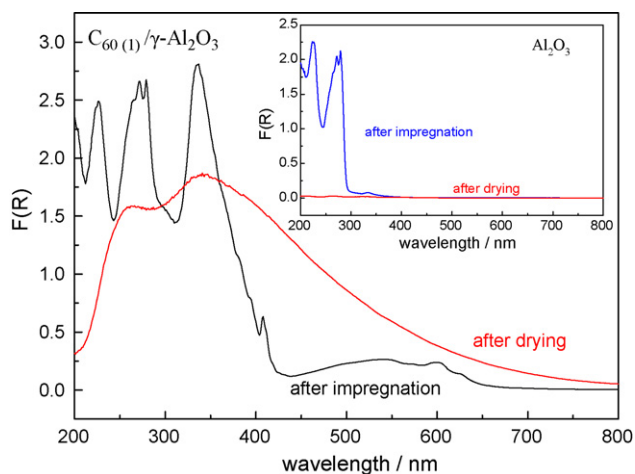
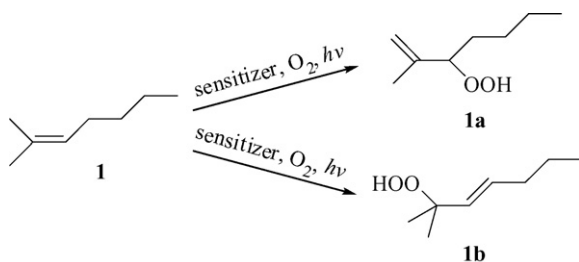


Fig. 8. DR spectra recorded for the sample $C_{60}(1)$ after each preparation step (see the text). The preparation step is indicated. Inset: DR spectra recorded after impregnation of the support with pure solvent (1,2-dichlorobenzene) and after heating at 180°C . The particular step is also indicated.

Fig. 8) and the dramatic change of the DR spectrum upon drying (Fig. 8).

3.7. Photocatalytic activity

The activity of the photocatalysts studied has been assessed by performing a series of photooxidation experiments in CH_3CN using 2-methyl-2-heptene (**1**) as a model substrate:



The activity curves obtained over the different photocatalysts studied are shown in Fig. 9. In these curves, the % conversion of **1** is plotted as a function of reaction time. When the model reaction was run in the presence of pure $\gamma\text{-Al}_2\text{O}_3$ an insignificant oxidation

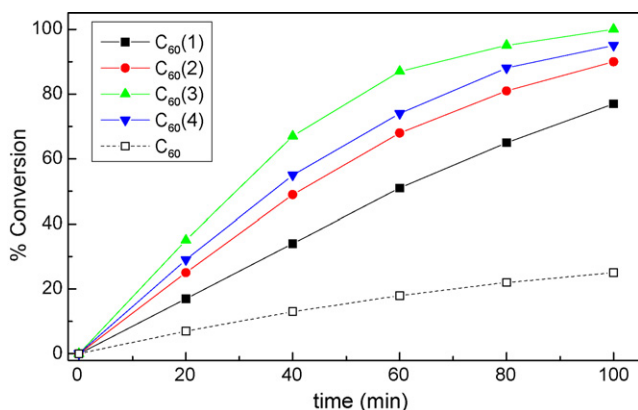


Fig. 9. Conversion of 2-methyl-2-heptene obtained at various reaction times over the catalysts studied. The corresponding values for unsupported C_{60} were also evaluated for comparison purposes. In this case the concentration of C_{60} in the reaction mixture was 2×10^{-4} M, corresponding to that involved in the suspension of the $C_{60}(4)$ photocatalyst.

was observed indicating that the $\gamma\text{-Al}_2\text{O}_3$ does not interfere to the photocatalyzed reaction. We have also verified that no oxidation products were obtained when blank experiments were run in the absence of light or catalyst.

It may be observed that under the conditions explored, substrate conversion is achieved in the range of 71–99% for 100 min of irradiation. More importantly, it may be seen that the activity of the alumina-supported catalysts is much higher than that obtained for the unsupported C_{60} . For example, the percentage conversions obtained after 100 min of irradiation over the $C_{60}(4)$ and C_{60} photocatalysts were found to be equal to 95 and 25%, respectively. It should be mentioned that the same amount of C_{60} is involved in both cases.

In all cases the allylic hydroperoxides **1a** and **1b** were obtained in a 1:1 molar ratio. Moreover, the photooxidation of **1** in the presence of well-established $^1\text{O}_2$ sensitizers, such as rose bengal (RB) or tetraphenyl porphyrine (TPP) afforded **1a** and **1b** in the same ratio. This result is indicative of a $^1\text{O}_2$ formation as the reactive intermediate in the case of the C_{60} mediated heterogeneous photooxidation of **1**. Further experiments performed with the addition in the reaction mixture of 5 mg of 1,4-diazabicyclo[2.2.2]octane, an excellent $^3C_{60}^*$ and $^1\text{O}_2$ quencher [44,45], revealed an almost complete inhibition of the $C_{60}/\text{Al}_2\text{O}_3$ -sensitized photooxidation of **1**.

Furthermore, it may be seen that the increase of the C_{60} loading, upon going from $C_{60}(1)$ to $C_{60}(2)$ and $C_{60}(3)$, is reflected in the increase of the photocatalytic activity of the corresponding $C_{60}/\text{Al}_2\text{O}_3$ catalyst. On the other hand, the photocatalytic activity of $C_{60}(4)$ sample did not follow the same trend, and surprisingly, exhibited a slightly lower activity than that of the $C_{60}(3)$ catalyst. Thus, from the practical viewpoint, this work shows that using a $C_{60}/\gamma\text{-Al}_2\text{O}_3$ photocatalyst with a C_{60} content of about 3% (w/w) one may obtain the maximum catalytic activity. The increase in the activity up to 3% (w/w) seems to follow approximately the increase in the surface exposed by the supported C_{60} (Fig. 4). Apparently, this increased surface provides more active sites for photocatalytic generation of $^1\text{O}_2$, thus resulting in enhanced oxidation of 2-methyl-2-heptene (**1**). However, the increase in the C_{60} surface observed in Fig. 4 cannot explain the inversion in the activity observed over the sample with the maximum C_{60} content ($C_{60}(4)$). The “volcano” like trend observed in the activity, expressed as a percentage conversion of (**1**), implies that the intrinsic activity of each site is not constant but depends on the C_{60} loading. In order to investigate further this point we have calculated the turnover number (TON) and the turnover frequency (TOF). The variation of these parameters with time is illustrated in Fig. 10a and b, respectively. It may be seen that in all cases the TON and TOF values decrease as the C_{60} content increases. Therefore, intrinsic activity follows the opposite trend to that followed by the number of the active sites, and this may rationalize the observed volcano like trend observed in the % conversion values.

We could attribute the decrease in the intrinsic activity with the C_{60} content in the photocatalysts to both the decrease in the “supported C_{60} –alumina” interactions, manifested by photoluminescence (Fig. 6) and differential TGA (Fig. 7), and/or the decrease in the C_{60} dispersion (Fig. 4). Further studies, however, are necessary before the role of these interrelated parameters on the intrinsic catalytic activity can be confirmed.

3.8. Stability under working conditions and reusability of the catalysts

The catalyst over which the maximum conversion has been observed, that is $C_{60}(3)$, was selected as representative example. To test the catalysts’ stability, a solution of $C_{60}(3)$ (3.6 mg in 1 mL CH_3CN ca. 1.5×10^{-4} M C_{60}) was irradiated for 100 min under

continuous oxygen bubbling at 0–5 °C. The catalyst was kept in suspension by magnetic stirring. After irradiation the suspension was centrifuged and the supernatant solution was subjected to UV/vis spectral analysis indicating that no C₆₀ had been released into the solution. This result indicates that the contribution of the homogeneous reaction to the heterogeneously catalyzed reaction is actually negligible and confirms the aforementioned finding that quite strong chemical interactions developed between supported C₆₀ and the γ -Al₂O₃ surface upon heating at 180 °C. To further confirm our results on the leaching of the catalysts, C₆₀(3) was mixed with acetonitrile in a separate experiment and stirred for 2 h at 22 ± 1 °C. Then the catalyst was filtered-off and 2-methyl-2-heptene (**1**) was added into the filtrates (0.03 M). The resulting solution was irradiated for 100 min in the presence of molecular oxygen. Only a small amount of hydroperoxides **1a** and **1b** (ca. 4%) was detected by gas chromatography. The above control experiment corroborates the previous conclusion that leaching did not result in any considerable removal of the supported C₆₀ from the support surface. As expected, in view of the negligible solubility of C₆₀ in CH₃CN [46], the leaching of C₆₀ sensitizer into the reaction solution is not favoured in this solvent. On the other hand, when the same experiments were carried out in hexane or CHCl₃, instead of CH₃CN, it was found that a considerable amount of C₆₀ had been lost from the alumina surface. In particular, the UV/vis spectra of the supernatant solutions were compared with a standard solution of C₆₀ (4.5 × 10⁻⁵ M C₆₀ in CHCl₃ or 3.5 × 10⁻⁵ M C₆₀ in hexane), indicating that 20% and 30% of C₆₀ catalyst had been lost from the alumina surface, when hexane or CHCl₃ was used as the reaction solvent, respectively. Accordingly, polar solvents such as acetonitrile are the most suitable for maintaining strictly heterogeneous conditions.

Reusability is one of the most important advantages of heterogeneous catalysts and its study may also provide important insights

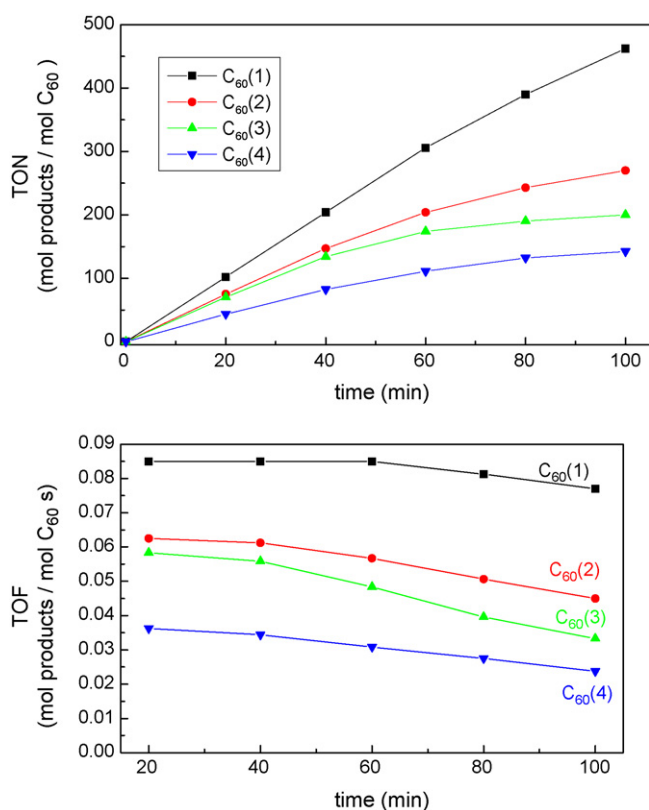


Fig. 10. TON, and TOF values achieved at various reaction times over the catalysts studied.

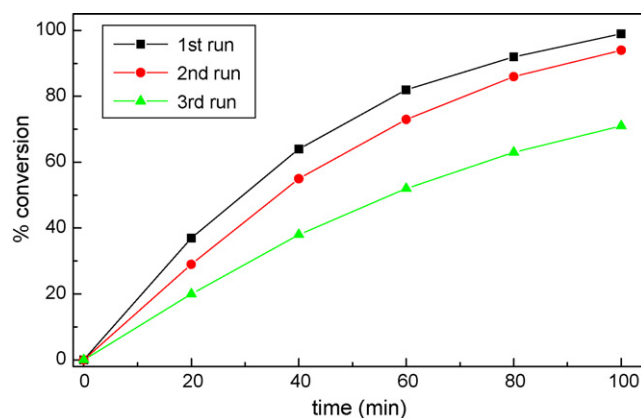


Fig. 11. Catalytic performance of recycled C₆₀(3) photocatalyst in the heterogeneous photooxidation of 2-methyl-2-heptene. The various runs are indicated.

into the catalyst stability during the catalytic cycle. Herein, the C₆₀(3) catalyst performance has been evaluated in three consecutive runs, to verify its potential recycling. Thus, **1** (0.03 M) was irradiated for 100 min in the presence of 3.6 mg C₆₀(3) (1.5 × 10⁻⁴ M C₆₀) in oxygen saturated CH₃CN, at 0–5 °C. The resulting solution was centrifuged, the supernatant was removed, and the solid catalyst was rinsed thoroughly four times with CH₃CN. The catalyst was then reused in the presence of 0.03 M of (**1**). The initial conversion of **1** at 100 min of irradiation, decreased slightly from 99 to 94%. When the catalyst rinsed again with CH₃CN followed by the addition of 0.03 M (**1**), an efficient oxidation was performed for a third time with 71% conversion (Fig. 11) indicating that the catalyst was gradually deactivated over time. A reasonable explanation for this effect is that the contact of the solid catalyst with the liquid phase brings about a progressive decrease in the ‘supported C₆₀–support’ interactions, thereby reducing the active surface.

3.9. Effect of catalyst amount on the photocatalytic activity

The dependence of the photocatalytic activity on the amount of catalyst was also investigated. The results from the time-course of the conversion of **1** with various amounts of catalyst are shown in Fig. 12. Typically, a higher concentration of the supported C₆₀ in the reaction mixture is expected to increase the percentage conversion. Indeed, it can be seen from Fig. 12 that as the catalyst concentration was increased, the oxidation rate was enhanced. In particular, using the catalyst concentration of 0.5 × 10⁻⁴ M C₆₀ (1.2 mg of C₆₀(3)), the time required for 80% completion of reaction was 80 min, whereas using 2.0 × 10⁻⁴ M C₆₀ (4.8 mg of C₆₀(3)) it was only 40 min. On the

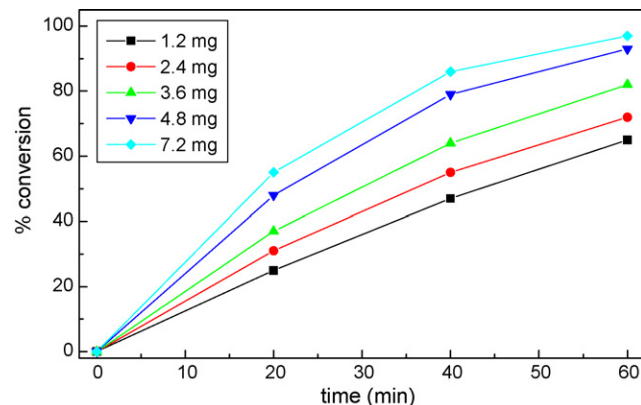


Fig. 12. Time profiles of the 2-methyl-2-heptene photooxidation catalyzed by C₆₀(3) in oxygen saturated CH₃CN at 0–5 °C.

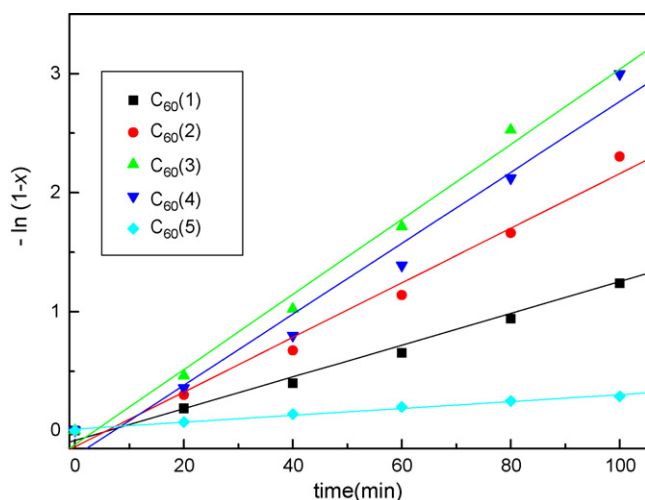


Fig. 13. Plots of Eq. (7) for the photooxidation of 2-methyl-2-heptene over the unsupported C_{60} and the $C_{60}(x)$ photocatalysts.

other hand, another interesting phenomenon was observed: the increase in the catalyst concentration beyond 2.0×10^{-4} M C_{60} did not affect the rate of the oxidation reaction as dramatically as in the lower concentration region. For example, essentially no increase of the oxidation rate was observed, upon going from 4.8 to 7.2 mg of $C_{60}(3)$ (2.0×10^{-4} and 3.0×10^{-4} M C_{60} , respectively). Thus, when the concentration value of the active phase was 2.0×10^{-4} M C_{60} , the reaction conversion reached almost the maximum value. We could attribute this observation to shadow effects. In fact, as the amount of the solid catalyst increased in the reaction mixture, a continuously higher fraction of the catalyst particles could not be illuminated being in the shadow of the particles suspended in front of them.

3.10. Formal kinetics

In order to investigate further the photocatalytic behavior of the $C_{60}(x)$ catalysts we studied the formal kinetics of the photooxidation of 2-methyl-2-heptene. The following equation may be written which relate the reaction time (t), the rate constant (k) and the conversion of 2-methyl-2-heptene (x):

$$k \cdot t = -\ln(1-x) \quad (8)$$

The above equation may be derived assuming first order dependence of reaction rate on the alkene concentration and taking into account that during the photocatalytic reaction the oxygen concentration in the reaction mixture remained constant. The linear dependence of the “ $-\ln(1-x)$ ” on “ t ” observed in all cases (Fig. 13) confirms the aforementioned assumption and indicates that the same kinetics is followed over the unsupported and supported C_{60} .

The values of the rate constant per gram of the catalyst were calculated by the slope of the linear curves and then the corresponding values per mmol of the supported C_{60} .

Table 2
Values of the rate constant (k) calculated per gram of the catalyst and per mmol of the supported C_{60} .

Catalysts	k ($g_{cat} \text{ min}^{-1}$)	k ($mmol_{C60} \text{ min}^{-1}$)
$C_{60}(1)$	3.6	260
$C_{60}(2)$	6.4	230
$C_{60}(3)$	8.9	213
$C_{60}(4)$	8.3	150

As expected, the first values follow the trend followed by the % conversion whereas the latter values follows the trend followed by TON or TOF (Table 2).

4. Conclusions

In conclusion, we have demonstrated the application of the simple and successive incipient wetness impregnation technique for successful immobilization of varying amounts of [60]fullerene on the $\gamma\text{-Al}_2\text{O}_3$ surface. It was found that a large portion of the supported C_{60} is comprised from C_{60} clusters or very small C_{60} aggregates. The remained portion of the supported C_{60} is comprised from aggregates of progressively increasing size. This non-uniform size distribution is reflected to a non-uniform distribution concerning the ‘supported phase–support’ interactions. The high and quite stable surface exposed by the supported C_{60} increases with the amount of the supported C_{60} , while the dispersion of the supported C_{60} decreases. The photocatalysts prepared may be safely used up to 200 °C.

All catalysts exhibited good conversion, turnover number and turnover frequency values, under mild reaction conditions in the heterogeneous oxidation of olefins via a $^1\text{O}_2$ ene reaction. The catalytic activity, expressed as % substrate conversion, increases with the amount of the supported C_{60} up to a value of 3% (w/w) and then decreases. The intrinsic activity expressed in TON or TOF decreases monotonically as the amount of the supported C_{60} increases. The aforementioned catalytic behavior was attributed to the opposite trends which follow the surface exposed by the supported C_{60} on one hand and the ‘supported C_{60} –support’ interactions and the C_{60} dispersion on the other hand. The first parameter increases with the C_{60} content, while the second and third parameters decrease.

The easy separation of the solid catalyst from the reaction mixture, the high dispersion of the supported C_{60} , the high activity and stability as well as the retained activity in subsequent catalytic cycles, make these supported catalysts suitable for a small-scale synthesis.

Acknowledgment

The Greek National Scholarships Foundation (IKY) is acknowledged for providing a three year fellowship to M.D.T.

References

- [1] A.A. Frimer (Ed.), Singlet Oxygen, vols. 1–4, CRC Press, Boca Raton, FL, 1985.
- [2] C. Schweitzer, R. Schmidt, Chem. Rev. 103 (2003) 1685–1757.
- [3] M. Prein, W. Adam, Angew. Chem. Int. Ed. Engl. 35 (1996) 477–494.
- [4] M. Stratakis, M. Orfanopoulos, Tetrahedron 56 (2000) 1595–1615.
- [5] C. Cantau, T. Pigot, N. Manoj, E. Oliveros, S. Lacombe, Chem. Phys. Chem. 8 (2007) 2344–2353.
- [6] E.L. Clennan, A. Pace, Tetrahedron 61 (2005) 6665–6691.
- [7] M.N. Alberti, M. Orfanopoulos, Tetrahedron 62 (2006) 10660–10675.
- [8] J.W. Arbogast, A.P. Darmanyan, C.S. Foote, F.N. Diederich, R.L. Whetten, Y. Rubin, M.M. Alvarez, S.J. Anz, J. Phys. Chem. 95 (1991) 11–12.
- [9] M. Terazima, N. Hirota, H. Shinohara, Y. Saito, J. Phys. Chem. 95 (1991) 9080–9085.
- [10] M. Orfanopoulos, S. Kambourakis, Tetrahedron Lett. 35 (1994) 1945–1948.
- [11] H. Tokuyama, E. Nakamura, J. Org. Chem. 59 (1994) 1135–1138.
- [12] M. Orfanopoulos, S. Kambourakis, Tetrahedron Lett. 36 (1995) 435–438.
- [13] T.W. Ebbesen, K. Tanigaki, S. Kuroshima, Chem. Phys. Lett. 181 (1991) 501–504.
- [14] M.R. Fraelich, R.B. Weisman, J. Phys. Chem. 97 (1993) 11145–11147.
- [15] Y. Kajii, T. Nakagawa, S. Suzuki, Y. Achiba, K. Obi, K. Shibuya, Chem. Phys. Lett. 181 (1991) 100–104.
- [16] Q. Xie, E. Perez-Cordero, L. Echegoyen, J. Am. Chem. Soc. 114 (1992) 3978–3980.
- [17] Y. Ohsawa, T. Saji, J. Chem. Soc. Chem. Commun. (1992) 781–782.
- [18] J.W. Arbogast, C.S. Foote, M. Kao, J. Am. Chem. Soc. 114 (1992) 2277–2279.
- [19] M.D. Tzirakis, M. Orfanopoulos, Org. Lett. 10 (2008) 873–876.
- [20] M.D. Tzirakis, M. Orfanopoulos, J. Am. Chem. Soc. 131 (2009) 4063–4069.
- [21] Y. Long, Y. Lu, Y. Huang, Y. Peng, Y. Lu, S.-Z. Kang, J. Mu, J. Phys. Chem. C 113 (2009) 13899–13905.
- [22] J. Lin, R. Zong, M. Zhou, Y. Zhu, Appl. Catal. B: Environ. 89 (2009) 425–431.

- [23] F. Loske, R. Bechstein, J. Schütte, F. Ostendorf, M. Reichling, A. Kühnle, *Nanotechnology* 20 (2009), 065606/1-065606/5.
- [24] P.V. Kamat, M. Gevaert, K. Vinodgopal, *J. Phys. Chem. B* 101 (1997) 4422–4427.
- [25] W.C. Oh, A.R. Jung, W.B.J. Ko, *J. Ind. Eng. Chem.* 13 (2007) 1208–1214.
- [26] V.I. Makarov, S.A. Kochubei, I.V. Khmelinskii, *Chem. Phys. Lett.* 355 (2002) 504–508.
- [27] P.V. Kamat, *J. Am. Chem. Soc.* 113 (1991) 9705–9707.
- [28] D. Bonifazi, A. Salomon, O. Enger, F. Diederich, D. Cahen, *Adv. Mater.* 14 (2002) 802–805.
- [29] H. Fu, T. Xu, S. Zhu, Y. Zhu, *Environ. Sci. Technol.* 42 (2008) 8064–8069.
- [30] J. Vakros, G. Panagiotou, C. Kordulis, A. Lycourghiotis, G.C. Vougioukalakis, Y. Angelis, M. Orfanopoulos, *Catal. Lett.* 89 (2003) 269–273.
- [31] G.C. Vougioukalakis, Y. Angelis, J. Vakros, G. Panagiotou, C. Kordulis, A. Lycourghiotis, M. Orfanopoulos, *Synlett* (2004) 971–974.
- [32] M.D. Tzirakis, I.N. Lykakis, G.D. Panagiotou, K. Bourikas, A. Lycourghiotis, C. Kordulis, M. Orfanopoulos, *J. Catal.* 252 (2007) 178–189.
- [33] A.B. Smith, H. Tokuyama, R.M. Strongin, G.T. Furst, W.J. Romanow, B.T. Chait, U.A. Mirza, I. Haller, *J. Am. Chem. Soc.* 117 (1995) 9359–9360.
- [34] K.M. Creegan, J.L. Robbins, W.K. Robbins, J.M. Millar, R.D. Sherwood, P.J. Tindall, D.M. Kox, A.M. Smith, J.P. McCauley Jr., D.R. Jones, R.T. Gallagher, *J. Am. Chem. Soc.* 114 (1992) 1103–1105.
- [35] E. Ntararas, H. Matralis, G.M. Tsivgoulis, *Tetrahedron Lett.* 45 (2004) 4389–4391.
- [36] T.H. Gfoerer, in: R.A. Meyers (Ed.), *Encyclopedia of Analytical Chemistry*, John Wiley & Sons Ltd., Chichester, 2000, pp. 9209–9231.
- [37] M. Anpo, S. Dzwigaj, M. Che, *Adv. Catal.* 52 (2009) 1–42.
- [38] C. Reber, L. Yee, J. McKiernan, J.I. Zink, R.S. Williams, W.M. Tong, D.A.A. Ohlberg, R.L. Whetten, F. Diederich, *J. Phys. Chem.* 95 (1991) 2127–2129.
- [39] M. Muccini, *Synth. Met.* 83 (1996) 213–219.
- [40] T. Ohno, K. Matsuishi, S. Onari, *J. Chem. Phys.* 114 (2001) 9633–9637.
- [41] F. Zhang, Y. Fang, *J. Phys. Chem. B* 110 (2006) 9022–9026.
- [42] S. Liu, L. Zhang, Y. Fan, J. Luo, P. Zhang, *L. An, Appl. Phys. Lett.* 89 (2006), Art. Nub. 051911.
- [43] L. Vordonis, C. Kordulis, A. Lycourghiotis, *J. Chem. Soc. Faraday Trans. I* 84 (1988) 1593–1601.
- [44] D.M. Guldi, R.E. Huie, P. Neta, H. Hungerbühler, K.D. Asmus, *Chem. Phys. Lett.* 223 (1994) 511–516.
- [45] C.S. Foote, in: H.H. Wasserman, R.W. Murray (Eds.), *Singlet Oxygen*, Academic Press, New York, 1979, pp. 139–171.
- [46] R.S. Ruoff, D.S. Tse, R. Malhotra, D.C. Lorents, *J. Phys. Chem.* 97 (1993) 3379–3383.